

The influence of dark matter halo onto the evolution of a supermassive black hole

M. I. Zelnikov¹, E. A. Vasiliev²
Lebedev Physical Institute, Moscow

Abstract

The influence of dark matter (DM) on the growth of supermassive black holes (SMBHs) in galaxies is studied. It is shown that gravitational scattering of DM particles on bulge stars leads to diffusion of DM in phase space $\{m, m_z, I\}$. Appropriate diffusion coefficients are calculated for different bulge models, and it is argued that the diffusion along m axis is the most important effect. It is shown that this process leads to noticeable flow of DM into the black hole (BH), resulting in its power-law growth: $M_{bh} \propto t^{9/16}$. Comparison with observational data shows that, in principle, this effect may explain observed masses of SMBHs. Special attention is paid to the corrections related to the innermost region of BH gravitational influence and the diffusion along I axis. Their influence on the BH growth law is shown to be negligible in most cases.

1 Introduction

The interaction of a supermassive black hole in a galaxy center with dark matter halo was already much investigated [1, 2, 3]. There an adiabatic invariant approach was applied to obtain DM dynamics for different halo structure models. The initial halo profiles were taken to be self-similar (power-law) $\rho \sim r^{-\alpha}$ ($0 < \alpha < 2$), isothermal ($\rho \sim r^{-2}$) and NFW profiles ($\rho \sim \frac{\delta_c}{r/r_s(1+r/r_s)^2}$) [4]. In [1] the method of adiabatic invariant is used to calculate small changes in orbital parameters of particles caused by slow variation of gravitational potential due to the black hole growth. This approach has two drawbacks: absorption by BH is not taken into account, and appropriate change of DM distribution function is neglected. The latter means that the loss cone is always full, that leads to overestimation of dark matter flow.

¹zelnikov@lpi.ru

²eugvas@lpi.ru

More correct approach was used in [5, 6]. There the evolution of DM distribution function due to absorption by BH and changes in BH mass and loss cone parameters were considered consistently. The authors came to the conclusion that for current values of black hole masses the fraction of dark matter inside them is rather small.

The method was developed in [7], where the change of dark matter distribution function outside the loss cone due to diffusion in phase space was taken into account. It was demonstrated that this diffusion caused by gravitational scattering of DM particles on stars refills the loss cone effectively and determines the BH growth law. This effect was shown to give reasonable estimates for observed black holes masses.

The present work further develops the mentioned approach by accounting for three other factors: change of gravitational potential in the vicinity of black hole, modification of star distribution in this region, and the conditions under which the diffusion becomes effectively two-dimensional. The diffusion coefficients for all phase variables are calculated near the absorption boundary, and it is shown that the effects listed above in most cases play no significant role in the BH growth process.

1.1 Dark matter in galaxies

While the most part of matter in the Universe is now proved to be dark, the nature of the dark matter still remains unclear. In most models, however, the significant or dominant part of dark matter is taken to consist of cold dark matter (CDM), i.e. non-relativistic particles interacting only gravitationally. This leads to the absence of thermodynamical equilibrium in DM gas and the necessity of kinetic approach. Following this approach it was shown that the initial inhomogeneities in DM distribution grow and form spherically-symmetric structures – non-dissipative gravitational singularities (NGSs) of different scales, having the same internal structure. General analytic theory of NGS formation [8] (confirmed by numerical simulations [9]) predicts that all these structures have similar density profiles described by the following formula:

$$\rho(r) = A r^{-\xi}, \quad \xi = 12/7. \quad (1)$$

As initial inhomogeneities are not spherically symmetric, the particles of NGS possess angular momenta (though total angular momentum of NGS is zero). However, high degree of contraction at the nonlinear stage makes these

momenta relatively small compared to maximal possible angular momenta for corresponding orbital sizes. It turns out that angular momentum m of a particle is related to its radial action I by the formula: $m^2 = l_0^2 I^2$, where $I = \frac{1}{\pi} \int_{r_{min}}^{r_{max}} v_r(r) dr$ and $l_0 \simeq 0.1$ is a small parameter. In this case, the distribution function of DM in variables I, m, m_z has the following form:

$$f(I, m, m_z) = f_0 I^{1/8} \delta(m^2 - l_0^2 I^2) \quad (2)$$

The formation of NGS of galactic scale is followed by the formation of galaxy itself due to infall of baryonic matter into gravitational well of NGS, its subsequent cooling and formation of galactic structures – disc, bulge and halo. After this stage the total gravitational potential is no longer defined by DM; conversely, in the central region it is mainly directed by baryons. Galaxy formation process is slow enough as compared to the dynamical time of DM particles, so that the gravitational potential evolution is adiabatic. This fact ensures that radial action is integral of motion (adiabatic invariant). It is defined by the equation

$$I(E, m) = \frac{1}{\pi} \int_{r_-}^{r_+} dr \sqrt{2(E - \Psi(r)) - \frac{m^2}{r^2}}, \quad (3)$$

where r_-, r_+ are minimal and maximal distances of a DM particle from the center; $r_- \ll r_+$ due to small angular momentum ($m \ll I$).

Our main task is to study the central region of a galaxy – the bulge, which we may consider to be spherically symmetric. Under this assumption angular momentum is also conserved, and we obtain that the DM distribution function written in variables I, m, m_z does not depend on time. Spatial distribution of DM is given by relation

$$\rho(r) = (2\pi)^3 \frac{1}{4\pi r^2} \int_0^\infty dm \int_{-m}^{+m} dm_z \int_{\Omega} dE \frac{\sqrt{2}}{\pi} \frac{1}{2\sqrt{E - \Psi - \frac{m^2}{2r^2}}} f(E, m). \quad (4)$$

Here Ω is the energy interval where the expression under the radical sign is non-negative.

Let us assume that the density and the potential of the bulge have power-law profiles:

$$n(r) \propto r^{-(2-\alpha)}, \quad M_b(r) \propto r^{\alpha+1}, \quad \Psi(r) \propto r^\alpha.$$

Then one can show [1, 5] that the radial action may be approximated (with the accuracy better than 8%) in a factorised form

$$\begin{aligned} I &= I_0(r_+) C(\mu) , \quad \mu = \frac{m}{I_0} , \\ I_0 &= \sqrt{G M_b(r_+) r_+} , \\ C(\mu) &= \frac{\sqrt{2}}{\pi} \int_{\frac{r_-}{r_+}}^1 d\chi \left[\int_{\chi}^1 \xi^{\alpha-1} d\xi - \frac{\mu^2}{2} \left(\frac{1}{\chi^2} - 1 \right) \right]^{1/2} , \end{aligned} \quad (5)$$

where the function $C(\mu)$ at small argument μ is linear:

$$C(\mu) \approx C(0) - b_\alpha \mu , \quad C(0) > 0 , \quad b_\alpha \sim 1 . \quad (6)$$

Hence the DM density profile is also power-law:

$$\rho(r) = A' r^{-\xi'} , \quad \xi' = -\frac{15}{8} + \frac{9}{16}\alpha . \quad (7)$$

Let us now overview the bulge structure and proceed to estimation of DM fraction in bulge.

1.2 Bulge overview

Bulge is the central part of a galaxy, for our Galaxy its radius being about 1 kpc and mass about $10^{10} M_\odot$ [10]. We assume it to be spherically symmetric. Bulge density profile can be derived from the dependence of stars velocity dispersion on distance to galactic center; we take it to be power-law: $n(r) \propto r^{-(2-\alpha)}$. For isothermal bulge, i.e. having uniform velocity dispersion, $\alpha = 0$. Milky Way bulge may be approximated with velocity dispersion $\sigma \propto r^{1/4}$ for $r \leq 50$ pc [11], which corresponds to $\alpha = 0.5$.

It should be noticed that currently available observations of distant galaxies usually do not have enough resolution to derive velocity dispersion on scales less than a hundred parsecs [12]. We assume their bulges to be isothermal in central parts, but one can show that the exact form of the star density profile does not matter much; only its integral characteristics affect the final result.

Generally, in the center of a galaxy a compact object is located, which is assumed to be a supermassive black hole (for a recent review see [13]). For our own Galaxy it is now proved that this compact object Sgr A* is a black

hole with mass $M_{bh} \simeq 2.9 \cdot 10^6 M_\odot$ [14]. The innermost star cluster has the following density profile:

$$n(r) = n_0 \left(\frac{r}{r_0} \right)^{-3/2}, \text{ where } n_0 = 10^8 \frac{1}{\text{pc}^3}, \quad r_0 = 0.02 \text{ pc} [15]. \quad (8)$$

Hence the mass of this cluster is $M(r) = \int_0^r M_s n(r') 4\pi r'^2 dr' = \frac{8\pi}{3} M_s n_0 r_0^3 \left(\frac{r}{r_0} \right)^{3/2}$. Let us define the influence radius of a BH by the condition that the total mass of stars inside this radius equals that of the BH:

$$R_0 = \left(\frac{M_{bh}}{M_s} \frac{3}{8\pi n_0 r_0^{3/2}} \right)^{2/3} \approx 1 \text{ pc at the moment.} \quad (9)$$

So we may assume that inside this radius the gravitational potential is dominated by the BH, while outside it the influence of the BH is negligible.

Notice that BH and bulge evolution changes values of n_0 and R_0 , as well as the power-law index in inner cluster distribution (8). If we assume that the density is continuous at R_0 , then the following relation between M_{bh} and R_0 arises:

$$M_{bh} = \frac{8\pi}{3} M_s \tilde{\eta}_b R_0^{1+\alpha}. \quad (10)$$

Here $\tilde{\eta}_b$ is bulge constant entering the expression: $n_b(r) = \tilde{\eta}_b r^{-2+\alpha}$.

1.3 Dark matter in the bulge

The total mass of Milky Way's dark matter halo can be assessed to be $M_H \sim 10^{12} M_\odot$, its radius to be $R_H \sim 100$ kpc [8]. From (5) we derive adiabatic invariant for particles with $R_+ = R_H$ to be $I_{max} = 0.35(G M_H R_H)^{1/2}$, then total halo mass computed from initial distribution (2) is

$$M_H = \frac{8}{9} (2\pi)^3 f_0 I_{max}^{9/8}, \quad (11)$$

hence

$$f_0 = 3.5 \frac{1}{(2\pi)^3} \frac{M_H^{7/16}}{(G R_H)^{9/16}}. \quad (12)$$

The value of f_0 for our Galaxy is $6 \cdot 10^8 \text{ g} \left(\frac{\text{cm}^2}{\text{c}} \right)^{-9/8}$.

Now let's estimate the amount of DM inside the bulge:

$$\frac{M_{DM}}{M_B} = \frac{M_H}{(G M_H R_H)^{9/8}} \frac{(G M_B R_B)^{9/8}}{M_B} = \left(\frac{M_H}{M_B} \right)^{\frac{7}{16}} \left(\frac{R_B}{R_H} \right)^{\frac{9}{16}} \sim 1.$$

This means that initially the mass of dark matter inside bulge is comparable to the baryonic mass. The same estimation is valid for the innermost region (BH's domain of influence).

It is plausible that at the moment the amount of DM in bulge and, certainly, in its central region, is less than the amount of baryons due to processes of DM diffusion and absorption, which we shall discuss later. This implies that neglection of the DM potential is correct.

2 Problem definition and particle motion parameters

Our goal is to determine the possible fraction of DM in the BH, and to derive the growth law of the BH due to absorption of DM. Firstly, one can prove that the direct capture of particles with momenta less than $m_g = \frac{4GM_{bh}}{c}$ (non-relativistic absorption threshold) does not lead to significant growth of the BH, since their mass calculated from distribution (2) with current value of m_g is several orders of magnitude less than M_{bh} [6].

The simplest process which changes the distribution function of DM is gravitational scattering of DM particles on stars identical to Coulomb scattering in plasma.

2.1 Kinetic equation

The dark matter distribution function satisfies the following equation

$$\frac{\partial f(\vec{r}, \vec{v}, t)}{\partial t} + \{H_0, f\} = St\{f\}, \quad (13)$$

where H_0 is the Hamilton function for gravitational interaction, $St\{f\}$ is the collision term in Landau form:

$$St\{f\} = \frac{\partial}{\partial(\mu v_i)} \int \left[f(\vec{v}) \frac{\partial f'(\vec{v}')}{\partial(\mu' v'_j)} - f'(\vec{v}') \frac{\partial f(\vec{v})}{\partial(\mu v_j)} \right] B_{ij} d^3 v', \quad (14)$$

$$B_{ij} = \frac{2\pi G^2 \mu'^2 \mu^2 L_c}{|u|} \left(\delta_{ij} - \frac{u_i u_j}{u^2} \right).$$

Here entities with primes refer to stars and other to DM particles; particle and star masses are denoted as μ, μ' respectively, to avoid confusion with momentum. $\vec{u} = \vec{v} - \vec{v}'$ is the relative velocity, $L_c \sim 15$ is the Coulomb logarithm. Since $M_s \equiv \mu' \gg \mu$, we neglect the first term in equation:

$$St\{f\} = \frac{\partial}{\partial v_i} \left[W_{ij} \frac{\partial f}{\partial v_j} \right], \quad (15)$$

$$W_{ij} = 2\pi G^2 M_s^2 L_c \int \frac{u^2 \delta_{ij} - u_i u_j}{u^3} f'(\vec{v}', r) d^3 v'.$$

As soon as collision frequency of DM particles with stars is much less than their orbital motion frequency, one can rewrite the equation (13) in the form averaged over a period in action-angle variables $\{I_k, \phi_k\}$; $\{I_k\} = \{I, m, m_z\}$:

$$\frac{\partial f(\{I_k\}, t)}{\partial t} = St\{f\}. \quad (16)$$

Then the equation (15) for collision term looks as follows:

$$St\{f\} = \frac{\partial}{\partial I_k} \left[R_{kl} \frac{\partial f}{\partial I_l} \right], \quad (17)$$

$$R_{kl} = \frac{1}{(2\pi)^3} \int d^3 \phi \frac{\partial I_k}{\partial v_i} \frac{\partial I_l}{\partial v_j} W_{ij}. \quad (18)$$

Furthermore, observations show that the distribution function (DF) of stars may be considered as isotropic, i.e. not depending on momentum, even in the central region [14].

For isotropic DF the tensor W_{ij} takes the following form [7]:

$$W_{ij} = A(E, r) \delta_{ij} - B(E, r) \frac{v_i v_j}{v^2}, \quad (19)$$

$$A = \frac{16\pi^2}{3} G^2 M_s^2 L_c \int_{\Psi(r)}^{\infty} dE' f'(E') \begin{cases} 1 & , E \leq E' \\ \frac{3}{2} \frac{v'}{v} \left(1 - \frac{v'^2}{3v^2}\right) & , E > E' \end{cases}, \quad (20)$$

$$A - B = \frac{16\pi^2}{3} G^2 M_s^2 L_c \int_{\Psi(r)}^{\infty} dE' f'(E') \begin{cases} 1 & , E \leq E' \\ \left(\frac{v'}{v}\right)^3 & , E > E' \end{cases}. \quad (21)$$

From (5, 6) it follows that adiabatic invariant may be represented as follows:

$$I(E, m) \approx J(E) - b_\alpha m. \quad (22)$$

Note that in the case of Coulomb ($\alpha = -1$) and oscillator ($\alpha = 2$) potential the constant $b_\alpha = 1$, and in the case of isothermal potential (or close to it) $b_\alpha \approx 0.6$.

It is convenient to perform linear variable change: $\{I, m, m_z\} \rightarrow \{J, m, m_z\}$. Since it is linear, the expression (18) for tensor R_{kl} does not change. In addition, due to small value of parameter l_0 , the initial distribution function (2) has the same form in new variables:

$$f_i(J, m) = f_0 J^{1/8} \delta(m^2 - l_0^2 J^2). \quad (23)$$

The initial distribution function does not depend on m_z , hence the solution of kinetic equation (16) will not depend on m_z neither. So we can rewrite the expression (17) for collision term as follows:

$$St\{f\} = \frac{1}{m} \frac{\partial}{\partial m} m \left(R_{22} \frac{\partial f}{\partial m} + R_{12} \frac{\partial f}{\partial J} \right) + \frac{\partial}{\partial J} \left(R_{12} \frac{\partial f}{\partial m} + R_{11} \frac{\partial f}{\partial J} \right), \quad (24)$$

where the diffusion coefficients (18) are the following [7]:

$$\begin{aligned} R_{11} &= \left(\frac{\partial J}{\partial E} \right)^2 \langle (A - B)v^2 \rangle, \\ R_{12} &= \left(\frac{\partial J}{\partial E} \right) \langle (A - B)m \rangle, \\ R_{22} &= \left\langle A r^2 - B \frac{m^2}{v^2} \right\rangle. \end{aligned} \quad (25)$$

Here the averaging over angle variables is defined as

$$\langle X \rangle = \frac{2}{T} \int_{r_-}^{r_+} \frac{dr}{v_r} X, \quad (26)$$

$$T = 2 \int_{r_-}^{r_+} \frac{dr}{v_r}, \quad v_r = \sqrt{2(E - \Psi(r)) - \frac{m^2}{r^2}}, \quad (27)$$

where T is the particle oscillation period, v_r is its radial velocity.

Before proceeding to the solution of the kinetic equation (16, 24) one should define the distribution function of stars.

2.2 Distribution of stars

We assume that the density profile of stars in the bulge is power-law: $n(r) = n_0 \left(\frac{r}{r_0}\right)^{-\gamma}$, and the gravitational potential is also power-law $\Psi(r) = \Psi_0 r^\alpha$. In this case isotropic distribution function of stars can be written as a power-law dependence on energy [20]:

$$f'(v', r) = F_0 E^{-\beta}, \quad E = \frac{v'^2}{2} + \Psi(r), \quad (28)$$

$$\begin{aligned} n(r) &= \int_0^\infty f'(v', r) d^3 v' = \int_0^\infty F_0 \left(\frac{v'^2}{2} + \Psi_0 r^\alpha\right)^{-\beta} 4\pi v'^2 dv' \\ &= \frac{\Gamma(\beta - \frac{3}{2})}{\Gamma(\beta)} (2\pi)^{3/2} F_0 \Psi_0^{\frac{3}{2} - \beta} r^{\alpha(\frac{3}{2} - \beta)}, \text{ hence } \gamma = (\beta - \frac{3}{2})\alpha. \end{aligned} \quad (29)$$

We consider two particular cases: a) self-consistent potential of stars in the bulge (as known from observations, their density profile may be treated as power-law with power index close to 2[17]), and b) the central region of bulge where potential is dominated by the black hole.

In the first case we have:

$$\begin{aligned} \frac{d\Psi(r)}{dr} &= \frac{4\pi G M(r)}{r^2} = \frac{4\pi}{3 - \gamma} G M_s n_0 r_0^\gamma r^{1 - \gamma}, \text{ hence} \\ \Psi &= \Psi_0 r^\alpha, \quad \Psi_0 = \frac{4\pi G M_s n_0 r_0^\gamma}{(3 - \gamma)(2 - \gamma)}, \quad \gamma = 2 - \alpha, \end{aligned} \quad (30)$$

$$\sigma = \sigma_0 r^{\alpha/2} \text{ is the velocity dispersion, } \sigma_0^2 = \Psi_0 \frac{\alpha}{2(1 - \alpha)}, \quad (31)$$

$$f'(E) = F_0 E^{-\beta}, \quad F_0 = \frac{\alpha(\alpha + 1)}{4\pi G M_s (2\pi)^{3/2}} \frac{\Gamma(\beta)}{\Gamma(\beta - \frac{3}{2})} \Psi_0^{\frac{2}{\alpha}}, \quad \beta = \frac{2}{\alpha} + \frac{1}{2}. \quad (32)$$

In the limit $\alpha \rightarrow 0$ these expressions describe isothermal star cluster. Let us rewrite them in this particular case separately:

$$\Psi(r) = \Psi_0 \ln \frac{r}{r_0}, \quad \Psi_0 = 2\sigma_0^2, \quad \sigma_0 \text{ is the velocity dispersion,} \quad (33)$$

$$n(r) = n_0 \left(\frac{r}{r_0}\right)^{-2}, \quad n_0 r_0^2 = \frac{\sigma_0^2}{2\pi G M_s}, \quad (34)$$

$$f'(E) = F_0 \exp\left(-\frac{E}{\sigma_0^2}\right), \quad F_0 = n_0 (2\pi \sigma_0^2)^{-3/2}. \quad (35)$$

In the second case the particle dynamics is governed by the Coulomb potential of the black hole.

$$\Psi(r) = -\frac{G M_{bh}}{r} . \quad (36)$$

Restricting our consideration to the case $\gamma = -3/2$, following from observations [15], we obtain from (29) $\beta = 0$. Hence the distribution function does not depend on energy and equals F_0 at $E < 0$:

$$f'(E) = F_0 = \frac{3}{8\sqrt{2}\pi(G M_{bh})^{3/2}} \frac{3 M_{bh}}{8\pi M_s R_0^{3/2}} , \quad (37)$$

where M_{bh} and R_0 are related by (10).

2.3 Dark matter motion parameters

In this section we present the motion parameters for DM particles for practically important cases.

$$\begin{aligned} I(E, m) &= \frac{1}{\pi} \int_{r_-}^{r_+} \sqrt{2(E - \Psi(r)) - \frac{m^2}{r^2}} dr - \text{adiabatic invariant;} \\ I(E, 0) &\equiv J(E) , \quad r_{\pm} - \text{turnpoints;} \\ T(E, m) &= 2\pi \frac{\partial I}{\partial E} - \text{particle oscillation period;} \\ \frac{r_-}{r_+} &= \chi_{min} \ll 1 , \quad \frac{m}{J} = \mu \ll 1 . \end{aligned}$$

For power-law potential (30):

$$J(E) = C_\alpha \frac{\sigma_0 r_+^{1+\frac{\alpha}{2}}}{\sqrt{\pi}} , \quad C_\alpha = \frac{1}{\sqrt{\pi}} \int_0^1 d\chi \sqrt{\frac{4(1-\alpha)}{\alpha}} (1 - \chi^\alpha) \approx 1 - 0.8\alpha , \quad (38)$$

$$T(E) = C_\alpha \frac{1 + \frac{\alpha}{2}}{1 - \alpha} \frac{\sqrt{\pi} r_+^{1-\frac{\alpha}{2}}}{\sigma_0} , \quad (39)$$

$$r_+ = \left(\frac{E}{2\sigma_0^2} \frac{\alpha}{1 - \alpha} \right)^{1/\alpha} , \quad \chi_{min} = C_\alpha \sqrt{\frac{\alpha}{4\pi(1 - \alpha)}} \mu . \quad (40)$$

In the limit $\alpha \rightarrow 0$ we obtain formulas for isothermal potential (33):

$$J(E) = \frac{1}{\sqrt{\pi}} \sigma_0 r_+ , \quad (41)$$

$$T(E) = \sqrt{\pi} r_+ / \sigma_0 , \quad (42)$$

$$r_+ = r_0 \exp \left(\frac{E}{2\sigma_0^2} \right) , \quad \chi_{min} = \frac{0.25\mu}{\sqrt{1.3 - \ln \mu}} . \quad (43)$$

For Coulomb potential (36):

$$J(E) = \frac{1}{\sqrt{2}} \sqrt{G M_{bh} r_+} , \quad (44)$$

$$T(E) = \frac{\pi}{\sqrt{2}} \frac{G M_{bh}}{|E|^{3/2}} , \quad (45)$$

$$r_+ = \frac{G M_{bh}}{|E|} , \quad \chi_{min} = \frac{\mu^2}{2} . \quad (46)$$

3 The diffusion coefficients

Two opposite cases should be distinguished: for particles with apocenter distances $r_+(J) < R_0$ (R_0 is the radius of BH (10)) we calculate coefficients using Coulomb potential, and for other particles we use the expressions for self-consistent bulge potential (this corresponds to assumption that these particles pass the most part of orbital period outside the BH's domain of influence).

3.1 The diffusion coefficients for the bulge

Below we present the quantities A , $A - B$ for power-law (including isothermal) star distribution:

$$A = \frac{4}{3\sqrt{2\pi}} G M_s L_c \sigma(r) r^{-2} \cdot \tilde{A}_\alpha(\tilde{v}) , \quad \tilde{v} = \frac{v(r)}{\sigma(r)} , \quad (47)$$

$$A - B = \frac{4}{3\sqrt{2\pi}} G M_s L_c \sigma(r) r^{-2} \cdot \tilde{\Omega}_\alpha(\tilde{v}) , \quad (48)$$

where

$$\begin{aligned} \tilde{A}_\alpha(\tilde{v}) &= \left[\frac{(\tilde{v}^2/2\zeta + 1)^{-(\beta-1)}}{\beta-1} + \frac{\tilde{v}^2}{2\zeta} F \left(\frac{3}{2}, \beta; \frac{5}{2}; -\frac{\tilde{v}^2}{2\zeta} \right) - \frac{\tilde{v}^2}{10\zeta} F \left(\frac{5}{2}, \beta; \frac{7}{2}; -\frac{\tilde{v}^2}{2\zeta} \right) \right] \times \\ &\times \frac{\alpha(\alpha+1)\sqrt{\zeta}}{2} \frac{\Gamma(\beta)}{\Gamma(\beta - \frac{3}{2})} , \end{aligned}$$

$$\tilde{\Omega}_\alpha(\tilde{v}) = \left[\frac{(\tilde{v}^2/2\zeta + 1)^{-(\beta-1)}}{\beta-1} + \frac{\tilde{v}^2}{5\zeta} F\left(\frac{5}{2}, \beta; \frac{7}{2}; -\frac{\tilde{v}^2}{2\zeta}\right) \right] \times \frac{\alpha(\alpha+1)}{2} \frac{\sqrt{\zeta}}{\Gamma(\beta - \frac{3}{2})},$$

$$\zeta = 2 \frac{1-\alpha}{\alpha} = \frac{\Psi_0}{\sigma_0}, \quad F(.., ..; \dots; ..) \text{ is the hypergeometric function,}$$

and for isothermal profile

$$\begin{aligned} \tilde{A}_0(\tilde{v}) &= \frac{3}{2} \left[\frac{\exp(-\frac{\tilde{v}^2}{2})}{\tilde{v}^2} + \frac{\tilde{v}^2 - 1}{\tilde{v}^3} \Phi(\tilde{v}) \right], \\ \tilde{\Omega}_0(\tilde{v}) &= 3 \left[-\frac{\exp(-\frac{\tilde{v}^2}{2})}{\tilde{v}^2} + \frac{1}{\tilde{v}^3} \Phi(\tilde{v}) \right], \quad \Phi(x) = \int_0^x \exp(-\frac{t^2}{2}) dt \\ &\quad \text{is the probability integral.} \end{aligned}$$

The graphs of functions $\tilde{A}_\alpha(x)$, $\tilde{\Omega}_\alpha(x)$ are displayed on fig.1

Now let us calculate the diffusion coefficients R_{11} , R_{12} , R_{22} according to (25).

First of all, we are interested in low values of momentum, so we neglect the second term in R_{22} , which is $\sim \mu^2$ times smaller than the first one.

$$R_{22} = \frac{8}{3\sqrt{2\pi}} G M_s L_c r_+ T^{-1} \int_{\chi_{min}}^1 \frac{d\chi}{\tilde{v}} \tilde{A}(\tilde{v}), \quad \chi = \frac{r}{r_+} \quad (49)$$

$$\tilde{v} = \begin{cases} \sqrt{\frac{4(1-\alpha)}{\alpha}} \sqrt{\chi^{-\alpha} - 1} & , \quad \alpha > 0 \\ \sqrt{-4 \ln(\chi)} & , \quad \alpha = 0 \end{cases}.$$

We take the lower limit of integration in χ_{min} to be zero, since at low χ (high \tilde{v}) the integrand is small. Then we have for R_{22} the following expression:

$$R_{22} \approx 0.46 G M_s L_c \sigma_0^{\frac{1}{1+\alpha/2}} J^{\frac{\alpha}{2+\alpha}}. \quad (50)$$

This coincides with the value obtained in [7]. Note that R_{22} does not depend on m and weakly depends on J , not depending on J at all in isothermal case.

For R_{11} we have:

$$R_{11} = \frac{8}{3\sqrt{2\pi}} G M_s L_c r_+ T^{-1} \left(\frac{T \sigma_0 r_+^{\alpha/2-1}}{2\pi} \right)^2 \int_{\chi_{min}}^1 d\chi \chi^{-2+\alpha} \tilde{v} \tilde{\Omega}(\tilde{v}). \quad (51)$$

The integral diverges at lower limit, so we take the value (40) for χ_{min} . For the isothermal case ($\alpha = 0$) it is possible to obtain an asymptotic approximation

of this integral at low χ_{min} . Since $\tilde{\Omega}_0(\tilde{v}) \approx \frac{3\sqrt{\pi}}{\sqrt{2}\tilde{v}^3}$, the integral approximately equals $(-\chi_{min} \ln \chi_{min})^{-1} \sim 1/\mu$. A similar consideration for $\alpha > 0$ leads to an estimate of the integral $\sim \mu^{-1+2\alpha}$. The expression in brackets before the integral weakly depends on α and equals $1/2\sqrt{\pi}$ for $\alpha = 0$. Then

$$R_{11} \approx R_{22} \cdot 0.1 \left(\frac{J}{m} \right)^{1-2\alpha}. \quad (52)$$

The last coefficient R_{12} can be represented as $R_{22} \cdot K_\alpha(\mu)$, where $K_\alpha(\mu) \rightarrow 0$ at $\mu \rightarrow 0$. So one can neglect the term with R_{12} in (24) at low μ .

3.2 The diffusion coefficients for the central region

We restrict the calculation to the case when the density of stars $n(r) \propto r^{-3/2}$. Then

$$R_{22} = \frac{32\pi^2}{3\sqrt{2}} G^2 M_s^2 L_c F_0 r_+^3 |E|^{1/2} T^{-1} \int_{\chi_{min}}^1 \frac{\chi^2 d\chi}{\sqrt{\frac{1}{\chi} - 1}} \left(\frac{4}{5\chi} - \frac{1}{5} \right).$$

The integral weakly depends on χ_{min} at low χ_{min} and equals ≈ 1.14 . Finally, we have

$$R_{22} = 2.4G^{1/2} M_s M_{bh}^{-1/2} R_0^{-3/2} L_c J^2. \quad (53)$$

Comparing (53) with expression (50) for bulge, we conclude that they coincide at $J = J(R_0)$ (i.e. at the boundary of central region of the black hole influence). This means that the expressions for two limiting cases are consistent with each other.

$$R_{11} = \frac{16}{3\sqrt{2}} G^2 M_s^2 L_c F_0 r_+ |E|^{3/2} T \int_{\chi_{min}}^1 d\chi \sqrt{\frac{1}{\chi} - 1} \left(\frac{2}{5\chi} + \frac{3}{5} \right) \quad (54)$$

Here the integral approximately equals $0.8/\sqrt{\chi_{min}}$; so with the aid of (46) we obtain

$$R_{11} = R_{22} \cdot 0.25 \frac{J}{m}. \quad (55)$$

Similarly to the previous case we get that $R_{12} \simeq \text{const} R_{22} \frac{m}{J}$, so it can be neglected at low m .

3.3 Diffusion timescale estimates

One can easily see that for an equation $\frac{\partial f}{\partial t} = \frac{\partial}{\partial x}(A \frac{\partial f}{\partial x})$ the characteristic time of “equilibrium establishment” at spatial scale l equals $\tau \sim \frac{l^2}{8A}$. Let us make a few estimates for kinetic equation (16) with coefficients (50,52) calculated for the bulge.

The diffusion timescale for momenta $\tau_2 = \frac{(l_0 J_0)^2}{8R_{22}} \sim 10^6 \left(\frac{r_+}{1 \text{ pc}} \right)^2$ yr, so that the galactic age corresponds to spatial area of $r \leq 100$ pc. The coefficient R_{11} increases with decreasing m . The diffusion timescale along J axis at minimal momentum $m = m_g$ equals $\tau_1 \sim 3 \cdot 10^6 \frac{r_+}{1 \text{ pc}}$ yr, and for $r_+ \sim 100$ pc τ_1 is much less than the galactic age. But for momenta at least an order of magnitude greater than m_g the diffusion along J axis does not disturb much the one-dimensional diffusion along m . We will show in the next section that if we account for a cutoff of star distribution function at $r \rightarrow 0$, then we obtain a finite limit for R_{11} with decreasing m . Thus τ_1 becomes comparable with τ_2 or greater for all $r_+ \leq 100$ pc. Hence in the first approximation we can neglect the diffusion along J in comparison with the diffusion along m , at least for not very small values of m .

In addition we determine the characteristic timescale for diffusion in the central region. Since $R_{22} \sim J^2 = l_0^2 m^2$ the timescale does not depend on initial value of momentum and equals $\tau_2 = 10^6 \text{ yr} \times \left(\frac{M_{bh}}{3 \cdot 10^6 M_\odot} \right)^2$.

3.4 Diffusion coefficients for an improved star distribution

Indeed, in deriving relations (32,37) we have neglected the fact that the density of stars in the vicinity of a black hole may be significantly less than that follows from general power-law profile due to stars capture or tidal disruption by the black hole. From (51) we see that it is the stars in the pericenter of the orbit that affect the coefficient R_{11} most of all. Hence for particles with low momenta these are the innermost stars, which number we may have overestimated. Now let us try to evaluate corrections resulting from this fact.

Firstly, consider the Coulomb potential region. Observations show [16] that the nearest star’s orbital axis approximately equals $1000 \text{ AU} = 3 \cdot 10^{-4} \text{ pc}$. But from (8) we see that the number of stars inside a sphere of radius 1000 AU should be about 15.

For correction we adopt that stars distribution function vanishes for energies $E < E_{cr} = -\frac{GM_{bh}}{r_{cr}}$. Thus the density profile (8) transforms to

$$n(r) = n_0 \left(\frac{r}{r_0} \right)^{-3/2} \left[1 - \left(1 - \frac{r}{r_{cr}} \right)^{3/2} \right]. \quad (56)$$

Comparison with observations gives the value $r_{cr} \simeq 5 \cdot 10^{-3}$ pc $\sim 10^4 r_g$.

Now let us calculate modified coefficient R_{11} . Following (54) we obtain the expression (with integration from 0 to 1 in this case):

$$R_{11} = \frac{16}{3\sqrt{2}} G^2 M_s^2 L_c F_0 r_+ |E|^{3/2} T \begin{cases} \left(\frac{3\pi}{4} - \frac{\pi}{4} \chi_{cr} \right) / \sqrt{\chi_{cr}} & , \chi_{min} < \chi_{cr} < 1 \\ \frac{\pi}{2\chi_{cr}} & , \chi_{cr} > 1 \end{cases} . \quad (57)$$

$$\chi_{cr} = \frac{r_{cr}}{r_+} .$$

For $r_+ < 1$ pc, $\mu = \frac{m}{T} \leq 0.1$, we have $\chi_{cr} > \chi_{min}$, hence in the whole central region of Coulomb potential the lower limit of integration R_{11} is given by χ_{cr} . This means that R_{11} is in fact is much less (approximately $\frac{1}{3} \sqrt{\chi_{cr}/\chi_{min}}$ times) than calculated from (55).

Secondly, the same formalism in the region of self-consistent (particularly, isothermal) potential should include the statement that the distribution function of stars vanishes at sufficiently low energies. For isothermal star distribution this corresponds to well-known solution for isothermal sphere with a core (i.e. no central cusp), and the core radius is of the order of r_{cr} . Unfortunately, we can make no estimate for the core radius from observations, since their spatial resolution is not enough. We may adopt the same value as calculated for our Galaxy ($r_{cr} \sim 10^2 \div 10^4 r_g$). One can show that this assumption changes the lower limit of integration in (51) to value $\chi_{min} \sim \max(r_-, r_{cr})/r_+$. Thus, R_{11} increases with decreasing momentum up to $m = (10^2 \div 10^3)m_g$ and then reaches constant limit. At the same time R_{22} is not affected by this cut since the integrand in (49) is small at small χ .

4 Dark matter absorption and growth of the black hole

4.1 One-dimensional diffusion approximation

It was shown in previous sections that coefficient R_{22} does not depend on m in the case of bulge; coefficient $R_{11} \sim R_{22} \left(\frac{J}{m}\right)^\epsilon$, $\epsilon \leq 1$, and $R_{12} \sim R_{22} \frac{m}{J}$. Since initially $m = l_0 J \ll J$, and our scope of interest lies in the domain of low momenta, we can take $m \ll J$ and disregard the term with R_{12} . Furthermore, from the same arguments it follows that $\frac{\partial f}{\partial J} \sim l_0 \frac{\partial f}{\partial m}$ at the initial instant, and since $R_{11} \sim R_{22}$ at $m = l_0 J$, then $R_{11} \partial f / \partial J \ll R_{22} \partial f / \partial m$ at not very low values of m . Finally, $f(m, J, t) = 0$ at $m = m_g$, hence $\frac{\partial f}{\partial J} \Big|_{m=m_g} = 0$, and $R_{11} \frac{\partial f}{\partial J}$ is limited at $m \rightarrow 0$. Also notice that in fact R_{11} itself is limited at $m \rightarrow 0$, as noted previously.

To summarize, in the first approximation we can leave in (24) only the first term and rewrite the kinetic equation (16) as follows:

$$\frac{\partial f}{\partial t} = \frac{1}{m} R(J) \frac{\partial}{\partial m} \left(m \frac{\partial f}{\partial m} \right) , \quad (58)$$

$$\text{with boundary conditions } f|_{m=m_g} = 0 , \quad m \frac{\partial}{\partial m} f|_{m=\infty} = 0 , \quad (59)$$

initial conditions (12) and diffusion coefficient

$$R(J) = 0.46 G M_s L_c \sigma_0^{\frac{1}{1+\alpha/2}} J^{\frac{\alpha}{2+\alpha}} \cdot \begin{cases} 1 & , \quad J > J_0(M_{bh}) \\ \left(\frac{J}{J_0}\right)^2 & , \quad J < J_0 \end{cases} . \quad (60)$$

$$\text{Here } J_0 = \sqrt{G M_{bh} R_0 / 2} \propto M_{bh}^{\frac{1+\alpha/2}{1+\alpha}} \quad (61)$$

is the boundary value separating the BH domain of influence and the bulge itself (as follows from (10, 44)).

The flux of dark matter through the surface $m = m_g$ is given by the expression

$$\begin{aligned} S(t) &= -(2\pi)^3 \iiint dJ dm dm_z \frac{\partial f}{\partial t} = -(2\pi)^3 \iint dJ dm 2m \frac{1}{m} R \frac{\partial}{\partial m} m \frac{\partial f}{\partial m} = \\ &= (2\pi)^3 \int dJ \cdot 2 \left(m R(J) \frac{\partial f}{\partial m} \right) \Big|_{m=m_g} = 2(2\pi)^3 \int dJ f_0 J^{1/8} S_J(t) , \end{aligned} \quad (62)$$

where $S_J(t) = m_g R \frac{\partial f}{\partial m}$ is the flux through $m = m_g$ for equation (58) with the initial condition

$$f(m, t = 0) = \delta(m^2 - m_0^2), \quad m_0 = l_0 J. \quad (63)$$

4.2 Flux in one-dimensional diffusion

Consider an auxilliary task: equation (58) with boundary conditions (59) and initial condition (63) and determine the flux $S_J(t) = m_g R \frac{\partial f}{\partial m}$.

The solution of eq.(58) may be represented as

$$f(m, t) = \int_0^\infty dm' G(m, m', t) f(m', 0), \quad (64)$$

$$G = \int_0^\infty d\lambda m' e^{-\lambda R t} Z_\lambda(m, m_g) Z_\lambda(m', m_g) \text{ is Green function,}$$

$$Z_\lambda(m, m_g) = \frac{J_0(\sqrt{\lambda} m_g) Y_0(\sqrt{\lambda} m) - J_0(\sqrt{\lambda} m) Y_0(\sqrt{\lambda} m_g)}{(J_0^2(\sqrt{\lambda} m_g) + Y_0^2(\sqrt{\lambda} m_g))^{1/2}}$$

is the orthogonal system of fundamental functions of the boundary problem (59), J_0 , Y_0 are Bessel functions of first and second kind of 0th order.

The initial conditions (63) give $f(m, t) = \frac{1}{2m_0} G(m, m_0, t)$.

One can easily show that

$$\frac{\partial}{\partial m} Z_\lambda(m, m_g) = \frac{2}{\pi m_g} \frac{1}{(J_0^2(\sqrt{\lambda} m_g) + Y_0^2(\sqrt{\lambda} m_g))^{1/2}}.$$

Then the flux

$$\begin{aligned} S_J(t) &= m_g R \frac{1}{2m_0} \int_0^\infty d\lambda m_0 e^{-\lambda R t} Z_\lambda(m_0, m_g) \left. \frac{\partial Z_\lambda(m, m_g)}{\partial m} \right|_{m=m_g} = \\ &= \frac{R H(x, y)}{\pi R t}, \quad H(x, y) = \int_0^\infty d\eta e^{-\eta} \frac{J_0(\sqrt{\eta} x) Y_0(\sqrt{\eta} y) - J_0(\sqrt{\eta} y) Y_0(\sqrt{\eta} x)}{J_0^2(\sqrt{\eta} x) + Y_0^2(\sqrt{\eta} x)}. \end{aligned}$$

Here we have changed the variables: $\eta = \lambda R t$, $x = m_g / \sqrt{R t}$, $y = m_0 / \sqrt{R t}$.

One can show by numerical integration that $H(x, y) \simeq Z(x, y) \exp(-\zeta y^2)$ at $y \geq x + 4$, $Z(x, y)$ weakly depends on its arguments, $\zeta \sim 5$. Hence $S_J(t) \propto \frac{1}{t} \exp(-\frac{m_0^2}{\zeta R t})$. To obtain exact form of the dependence, we apply the following trick.

The flux $S_J(t, m) = m R \frac{\partial f}{\partial m}$ is a continuous function of m ; in the region $m_g < m < m_0$ we may take it to be a constant independent of m (it is correct for values of t greater than certain t_0 when the width of peak of DF becomes comparable with m_0 , see fig.2). Let us denote $\kappa(t) = \left. \frac{\partial f(m, t)}{\partial m} \right|_{m=m_g}$, then we have

$$S_J(t) = m_g R \kappa(t), \quad f(m, t) = \int_{m_g}^m \frac{S_J}{R m'} \partial m' = m_g \kappa(t) \ln \frac{m}{m_g}. \quad (65)$$

As we have already noticed, $\kappa(t) \approx \frac{\Xi}{t} \exp\left(-\frac{m_0^2}{5Rt}\right)$, Ξ is a constant (fig. 3). $\kappa(t)$ reaches maximal value at the exponent argument equal to -1 ; its maximal value $K_{max} = \frac{\Xi 5R}{e m_0^2}$. To determine the value of Ξ we apply expression (65) for $m = m_0/2$; having found analytically $f_{max}(m_0/2) = \frac{\ln 2}{2m_0^2}$, we obtain $\Xi = \frac{e \ln 2}{10 m_g R \ln \frac{m_0}{2m_g}}$. Finally, the flux is

$$S_J(t) = \frac{e \ln 2}{10 \ln \frac{m_0}{2m_g}} \cdot \frac{1}{t} \exp\left(-\frac{m_0^2}{5R(J)t}\right) \quad (66)$$

The correctness of the above consideration is proved by numerical investigation of the problem. We also should notice that, in fact, the expression (66) slightly overestimates the flux at $t \geq \frac{m_0^2}{R(J)}$ (up to a factor of 1.5, see fig. 4).

4.3 Black hole growth law

Firstly, we neglect that in central region of Coulomb potential the coefficient $R(J)$ differs from the expression (50) and take $R(J) = R_\epsilon J^\epsilon$, $\epsilon = \frac{\alpha}{2+\alpha} \leq 0.2$. Substituting the obtained value (66) of $S_J(t)$ into the expression (62) for the total flux, we rewrite it as follows:

$$\int_0^\infty f_0 J^{1/8} \frac{0.18}{\ln \frac{l_0 J}{2m_g}} \frac{1}{t} \exp\left(-\frac{l_0^2 J^{2-\epsilon}}{5R_\epsilon t}\right). \quad (67)$$

The logarithm in the integrand varies slightly, so we approximate it to have a constant value ~ 10 .

$$S(t) = 8.9 f_0 H_\epsilon \frac{R_\epsilon^{\frac{9}{8(2-\epsilon)}}}{t^{1-\frac{9}{8(2-\epsilon)}}}, \quad H_\epsilon = \left(\frac{5}{l_0^2}\right)^{\frac{9}{8(2-\epsilon)}} \frac{\Gamma(\frac{9}{8(2-\epsilon)})}{2-\epsilon}. \quad (68)$$

Supposing that black hole growth is governed only by the absorption of dark matter, we obtain the following growth law for the BH mass (assuming the mass of the seed black hole to be small):

$$M_{bh}(t) = B (R_\epsilon t)^{\frac{9}{8(2-\epsilon)}} , \quad B = 8.9 f_0 H_\epsilon^{\frac{8(2-\epsilon)}{9}} \quad (69)$$

Notice that more precise expression for $S_J(t)$ at large t reduces the value of B approximately 1.2 times.

Thus the black hole growth is power-law with power index about 9/16. This is in good agreement with previous work [7], though the power index is a bit lower.

4.4 Influence of the central region onto the black hole growth

One could suppose that the diffusion goes slower in the central region since the diffusion coefficient is lower there, and it may affect total growth law. In fact, nevertheless, it is not true. As has been shown in §3.3, the characteristic timescale for diffusion $\tau \propto M_{bh}^{-2}$ and is about 10^6 yr at the moment, hence it was even lower previously. Additionally, from (66) one can see that maximum of the flux goes from inside the region $J_{max} \leq \sqrt{5Rt/l_0^2}$, which at the moment corresponds to spatial area $r \leq 100$ pc, and value of J_0 separating the central and outer parts of the bulge corresponds to $r \simeq 1$ pc. These two quantities depend on time in similar ways: $J_{max} \sim t^{1/2}$, $J_0 \sim M_{bh}(t) \sim t^{9/16}$, so the relation $J_0 \ll J_{max}$ was also true in the past.

One can show that if R varies in time, then we should take the following expression for $S_J(t)$:

$$S_J(t) = \frac{e \ln 2}{10 \ln \frac{m_0}{2m_g}} \cdot \frac{R(t)}{\int_0^t R(t') dt'} \exp \left(-\frac{l_0^2 J^2}{5 \int_0^t R(t') dt'} \right) \quad (66')$$

Since $R(t)$ decreases at $t > t_0(J) : J_0(t_0) = J$, and remembering that $t_0(J) \simeq 10^4 \frac{l_0^2 J^2}{(5R)} = 10^4 t_{max}(J)$, where $t_{max}(J)$ is the time of maximal flux, we conclude that this correction affects only the far “tail” of $S_J(t)$, and is practically unimportant for growth law.

4.5 Influence of two-dimensional diffusion onto the black hole growth

Now let's try to estimate the effect of diffusion along J axis, i.e. the correctness of one-dimensional approximation. We restrict our consideration to the case $\alpha = 0$ when $R_{22} = \text{const}$. Having obtained approximate solution for one-dimensional diffusion equation, we substitute it into initial equation (16) and calculate the first term

$$\eta = \frac{\partial}{\partial J} \left(R_{11} \frac{\partial f}{\partial J} \right) = \frac{\partial}{\partial J} \left(R_{22} 0.1 \frac{J}{m} \frac{\partial}{\partial J} \left\{ \frac{e \ln 2}{10 \ln \frac{l_0 J}{2m_g}} \frac{\ln \frac{m}{m_g}}{R_{22} t} \exp \left[-\frac{l_0^2 J^2}{5 R_{22} t} \right] \right\} \right).$$

Of special interest is the time $t \sim t_{max}$ corresponding to the maximum of the flux: $t_{max} = \frac{l_0^2 J^2}{5R}$. It appears that $\eta \propto t_{max} - t$:

$$\eta = \frac{\ln 2}{5 \ln \frac{l_0 J}{2m_g}} \frac{R_{22} \ln \frac{m}{m_g}}{l_0^2 J^3 m} \left(1 - \frac{t}{t_{max}} \right). \quad (70)$$

Now we have to compare η with the second term in (16) $\eta_m = \frac{1}{m} \frac{\partial}{\partial m} (m R_{22} \frac{\partial f}{\partial m})$. However, one can easily see that substituting (65) into this term makes it zero, since this approximate solution does not satisfy initial equation in the whole region $m > m_g$. To avoid this problem, we calculate the left-hand side of (58) $\eta_m = \frac{\partial f}{\partial t}$:

$$\eta_m = \frac{5 \ln 2}{2 \ln \frac{l_0 J}{2m_g}} \frac{R_{22} \ln \frac{m}{m_g}}{l_0^4 J^4} \left(1 - \frac{t}{t_{max}} \right). \quad (71)$$

Comparing with (70) we obtain $\frac{\eta}{\eta_m} = \frac{2 l_0^2 J}{25 m}$.

For $J(r_+ = 100)$, $m = m_g$ this ratio is about 30. However, it was shown at the end of §3.4 that to estimate maximal value of R_{11} one should take $m \sim 10^2 m_g$ instead of $m = m_g$, which lowers this ratio to about unity.

It should be emphasized that all these estimates are rather approximate, since for precise assertions one should know the exact solution of the one-dimensional diffusion equation. The arguments of §4.2 give only the correct value for flux through $m = m_g$, but not the exact solution for all m .

In general case, the inapplicability of reduction to one-dimensional diffusion at $m \rightarrow m_g$ does not change much the value of flux through $m = m_g$,

since the diffusion along J axis leads to “blur” of distribution function along this axis, while the coefficient R_{22} only weakly depends on J as follows from (52). However, an especial consideration is necessary whether this diffusion may lead to the drift of dark matter into the region of large J where changes of m, J during one period exceed their values, and diffusion approximation becomes incorrect.

5 Comparison with observations and conclusions

In conclusion, we make theoretical estimates of black hole masses obtained from growth law (69) and compare them with observational data for several galaxies.

As it was noted previously, in distant galaxies it is difficult to measure the dependence of velocity dispersion on radius precisely. However, in galaxies M 31 and NGC 4258 it seems to be almost constant and equals approximately 200 km/s [18]. Taking the value of f_0 the same as in our Galaxy (12) and the time of growth $t = 3 \cdot 10^{17}$ s = 10^{10} yr we obtain the value $M_{bh} = 1.8 \cdot 10^7 M_\odot$. The observed black hole masses are $(2.0 \div 8.5) \cdot 10^7 M_\odot$ for M 31 and $3.8 \cdot 10^7 M_\odot$ for NGC 4258. The comparison shows that dark matter can comprise significant fraction of black hole masses in these galaxies.

As for Milky Way, the rotation curve is not flat in the center of the bulge, and the velocity dispersion may be approximately represented as $\sigma(r) = \sigma_0 \left(\frac{r}{10 \text{ pc}} \right)^{1/4}$, $\sigma_0 = 60$ km/s [11]. This corresponds to the value $\alpha = 0.5$. Then the expression (69) gives the black hole mass $M_{bh} \approx 10^7 M_\odot$, which clearly overestimates the adopted value of $M_{bh} \approx 2.9 \cdot 10^6 M_\odot$ [16] (about a factor of three). Notice that these values are about twice as smaller as in the work [7], because of more precise estimate of dark matter flow (68).

The disagreement with observations may be explained by rather rough estimates for quantities f_0 and l_0 , which are determined by the whole dark matter halo and are different for different galaxies. Another factor is the evolution of star distribution in bulge, including a possibility of similar diffusion of stars.

In conclusion, we can say that the model discussed can give reasonable estimate for observed masses of giant black holes in galactic centers. It is likely that a large fraction of black hole mass may be comprised of dark

matter.

Further development of this problem will require, firstly, more precise calculation of diffusion coefficients based on detailed data for star distribution in the central parts of the bulge; secondly, taking into account the bulge evolution; and finally, an exact consideration of two-dimensional diffusion accounting for particles Fermi-heating and their drift out of the bulge.

The authors are grateful to A.V. Gurevich, K.P. Zybin, A.S. Ilyin and V.A. Sirota for numerous fruitful discussions. This work was supported by RFBR grants 01-02-17829, 00-15-96697 and 03-02-06745.

References

- [1] P. Gondolo, J. Silk astro-ph/9906391.
- [2] J. D. MacMillan, R. N. Henriksen astro-ph/0201153.
- [3] P. Ullio, H. Zhao, M. Kamionkowski astro-ph/0101481.
- [4] J. Navarro, C. Frenk, S. White ApJ **490**, 493 (1997); astro-ph/9611107.
- [5] A. Gurevich Proc. IIIrd International Sakharov Conference (2002).
- [6] K. Zybin, A. Ilyin Proc. IIIrd International Sakharov Conference (2002).
- [7] A. Ilyin, K. Zybin, A. Gurevich Zh. eksp. teor. fiziki (in press) (2003); astro-ph/0306490.
- [8] A.V. Gurevich, K.P. Zybin Uspekhi fiz. nauk **165**, No.7 (1995).
- [9] L. Fukshige, J. Makino, ApJ **477**, L9 (1997).
- [10] M. Bureau ASP Conference series, Vol.III, 2002; astro-ph/0203471.
- [11] S. Tremaine et al. astro-ph/0203468.
- [12] S. Tremaine, K. Gebhardt et al. astro-ph/0203468;
- [13] J. Kormendy, K. Gebhardt astro-ph/0105230

- [14] R. Genzel astro-ph/0008119.
- [15] T. Ott, R. Schrödel, R. Genzel et al. The Messenger **111** (2003); astro-ph/0303408.
- [16] R. Schrödel, R. Genzel, T. Ott, A. Eckart astro-ph/0304197.
- [17] S.M. Faber et al., astro-ph/9610055.
- [18] Y. Sofue, V. Rubin Ann. Rev. Astron. Astrophys. **39** (2001); astro-ph/0010594.
- [19] J. Silk Int.J.Mod.Phys. A17S1 (2002) 167-179; astro-ph/0110404.
- [20] W. Saslaw "Gravitational physics of stellar and galactic systems", Cambridge Univ. Press, 1987

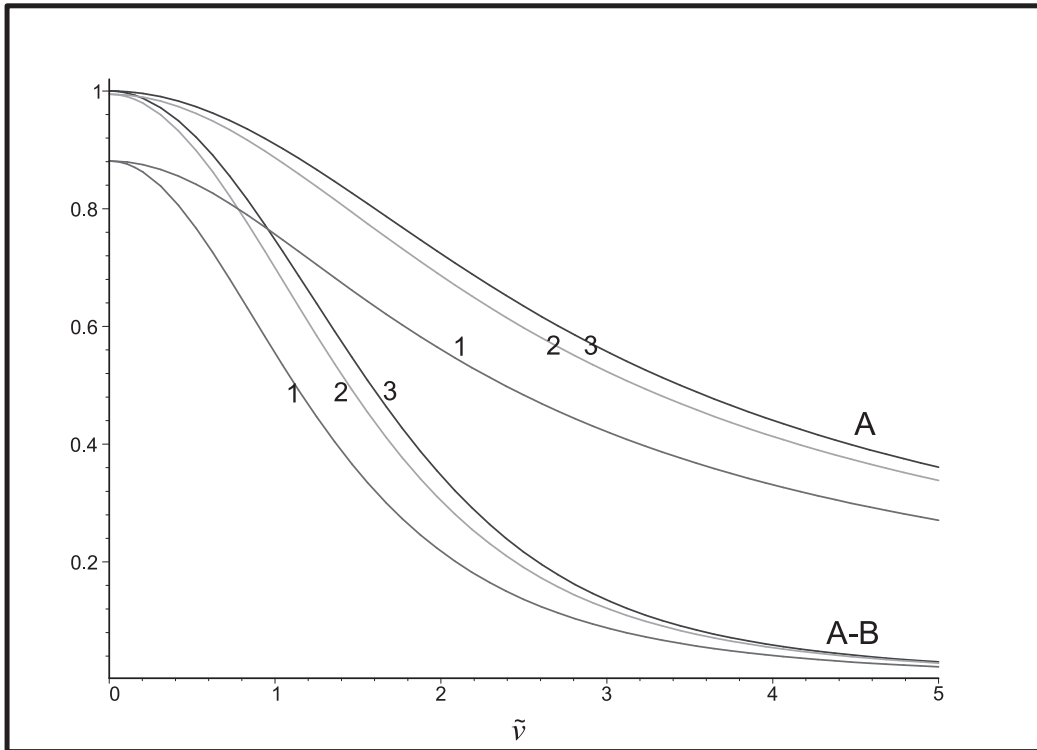


Figure 1: The graphs of functions $\tilde{A}(\tilde{v})$ (coefficient A , (47)), $\tilde{\Omega}(\tilde{v})$ (coefficient $A - B$, (47)) for different potentials: 1) power-law ($\Psi \propto r^\alpha$), $\alpha = 1/2$; 2) power-law, $\alpha = 1/4$; 3) isothermal ($\alpha = 0, \Psi \propto \ln r$).

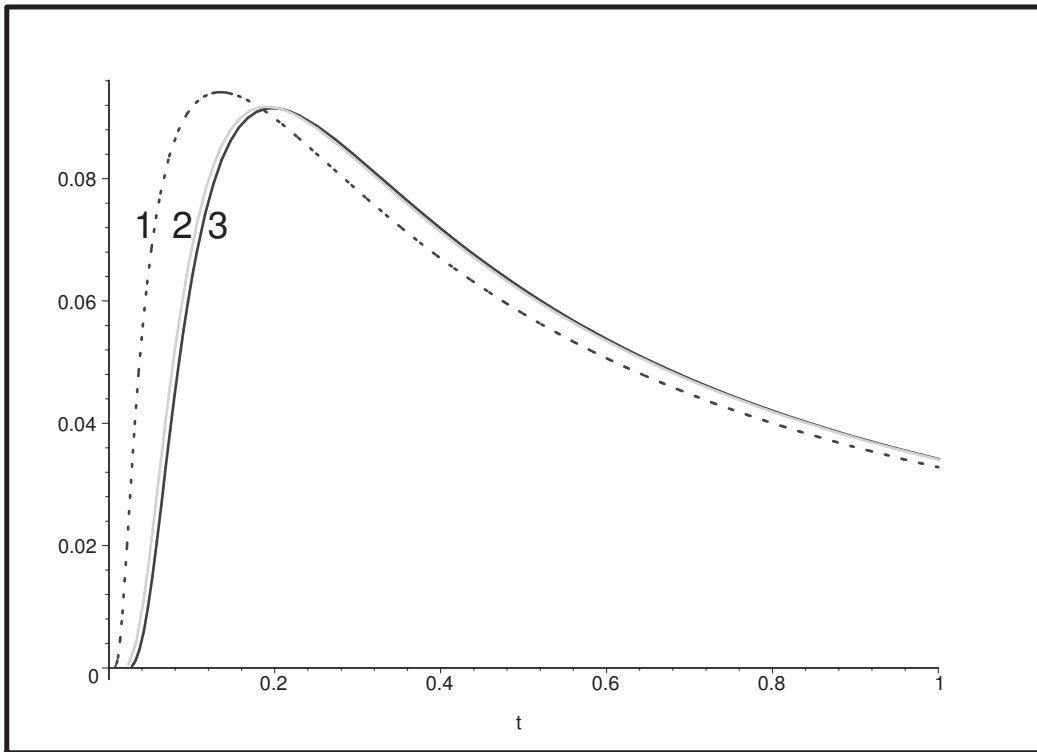


Figure 2: Normalized values $f(m, t) / \ln(m/m_g)$ for different m (65): 1) $m = m_0/2$, 2) $m = 20m_g$, 3) $m = 1.2m_g$. One can see that the graphs are quite similar, the normalized maximal values are approximately equal, though they are reached at different t .

The values are given for $m_0 = 100m_g$.

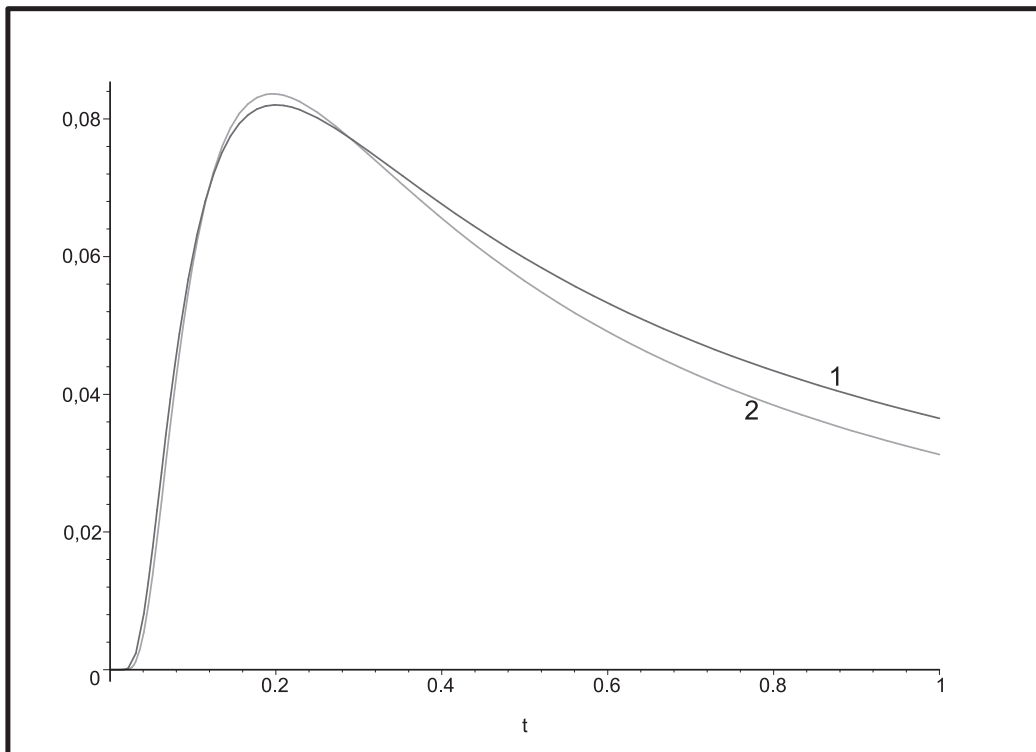


Figure 3: The flux function $\kappa(t)$: 1) theoretical (66), 2) obtained by numerical integration. One can see that the theoretical approximation is good enough for maximum of the flux, but overestimates it at large t .

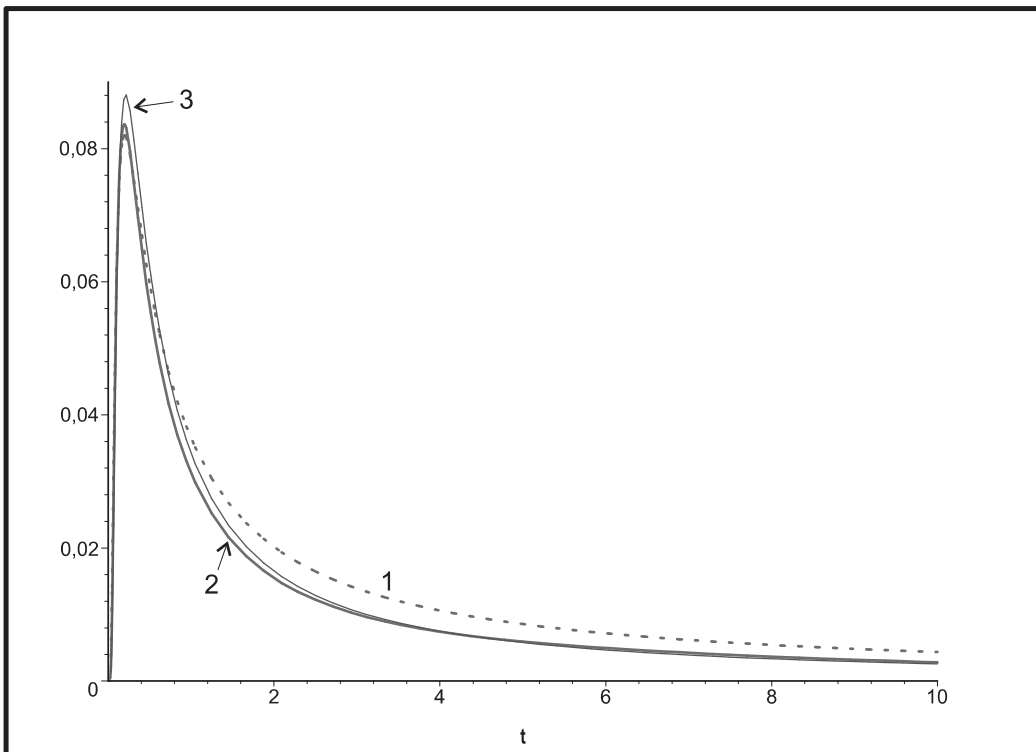


Figure 4: The corrected flux function $\kappa(t)$ for large t : 1) theoretical function (fig. 3), 2) obtained by numerical integration, 3) correcter theoretical function: $\kappa \propto t^{-5/4}$. The last approximation is much better.